





Article

Solvent-Free Synthesis of MIL-101(Cr) for CO₂ Gas Adsorption: The Effect of Metal Precursor and Molar Ratio

Kok Chung Chong^{1,2,*} , Pui San Ho¹ , Soon Onn Lai^{1,2}, Sze Shin Lee^{1,2}, Woei Jye Lau³ , Shih-Yuan Lu⁴ 
and Boon Seng Ooi⁵

¹ Department of Chemical Engineering, Lee Kong Chian Faculty of Engineering and Science, Universiti Tunku Abdul Rahman (UTAR), Jalan Sungai Long, Kajang 43000, Selangor, Malaysia; puisan2@utar.my (P.S.H.); laiso@utar.edu.my (S.O.L.); lsshin@utar.edu.my (S.S.L.)

² Centre for Photonics and Advanced Materials Research, Universiti Tunku Abdul Rahman (UTAR), Kampar 31900, Perak, Malaysia

³ Advanced Membrane Technology Research Centre (AMTEC), School of Chemical and Energy Engineering, Universiti Teknologi Malaysia, Johor Bahru 81310, Johor, Malaysia; lwoeijye@utm.my

⁴ Department of Chemical Engineering, National Tsing Hua University, Hsinchu 30013, Taiwan; sylu@mx.nthu.edu.tw

⁵ School of Chemical Engineering, Engineering Campus, Universiti Sains Malaysia, Seri Ampangan, Nibong Tebal 14300, Pulau Pinang, Malaysia; chobs@usm.my

* Correspondence: chongkc@utar.edu.my

Abstract: MIL-101(Cr), a subclass of metal–organic frameworks (MOFs), is a promising adsorbent for carbon dioxide (CO₂) removal due to its large pore volume and high surface area. Solvent-free synthesis of MIL-101(Cr) was employed in this work to offer a green alternative to the current approach of synthesizing MIL-101(Cr) using a hazardous solvent. Characterization techniques including XRD, SEM, and FTIR were employed to confirm the formation of pure MIL-101(Cr) synthesized using a solvent-free method. The thermogravimetric analysis revealed that MIL-101(Cr) shows high thermal stability up to 350 °C. Among the materials synthesized, MIL-101(Cr) at the molar ratio of chromium precursor to terephthalic organic acid of 1:1 possesses the highest surface area and greatest pore volume. Its BET surface area and total pore volume are 1110 m²/g and 0.5 cm³/g, respectively. Correspondingly, its CO₂ adsorption capacity at room temperature is the highest (18.8 mmol/g), suggesting it is a superior adsorbent for CO₂ removal. The textural properties significantly affect the CO₂ adsorption capacity, in which large pore volume and high surface area are favorable for the adsorption mechanism.

Keywords: metal–organic framework; MIL-101; solvent free; adsorption; carbon dioxide



Citation: Chong, K.C.; Ho, P.S.; Lai, S.O.; Lee, S.S.; Lau, W.J.; Lu, S.-Y.; Ooi, B.S. Solvent-Free Synthesis of MIL-101(Cr) for CO₂ Gas Adsorption: The Effect of Metal Precursor and Molar Ratio. *Sustainability* **2022**, *14*, 1152. <https://doi.org/10.3390/su14031152>

Academic Editors: Wei-Hsin Chen, Alvin B. Culaba, Aristotle T. Ubando and Steven Lim

Received: 10 December 2021

Accepted: 9 January 2022

Published: 20 January 2022

Publisher's Note: MDPI stays neutral with regard to jurisdictional claims in published maps and institutional affiliations.



Copyright: © 2022 by the authors. Licensee MDPI, Basel, Switzerland. This article is an open access article distributed under the terms and conditions of the Creative Commons Attribution (CC BY) license (<https://creativecommons.org/licenses/by/4.0/>).

1. Introduction

Energy demand is rapidly increasing, and world demand is expected to rise by another 19% in the coming twenty years, as the global population is growing simultaneously [1]. Currently, industrial power usage heavily depends on non-renewable energy produced by power plants, which are a major human source of CO₂ emission into the atmosphere [2]. It was reported that the CO₂ level in the atmosphere had unprecedentedly approached 417 ppm on average in 2020 [2], and had increased by around 45% since the mid-1800s, the start of the Industrial Revolution.

Energy is now in transition from non-renewable energy to clean energy sources, such as biomass. Wind energy is thought to be a solution for the world's energy supply, and an excellent solution for cutting down the emission of CO₂ gas into the atmosphere in the future. However, realizing and applying this clean energy source in industrial usage is challenging and will require many more years to accomplish [3]. Hence, capturing the excessive CO₂ emissions from industrial activities is the immediate action that needs to be

taken in order to minimize the environmental impact while also developing clean energy sources.

Carbon dioxide gas accounts for 60% of the greenhouse effect by trapping heat in the atmosphere. The Earth's average surface temperature has increased 1.18 °C since the start of the Industrial Revolution, attributed to global warming [4]. By the 22nd century, global sea levels are forecast to rise 30.5 to 121.9 cm and flood low-lying areas, an event mainly caused by melting ice in Antarctica and Greenland [4]. Additionally, the rising temperature of the Earth will affect wildlife habitats, leading to extreme weather change by increasing precipitation in some areas, while some regions will experience hot weather and drought [5].

Carbon capture and sequestration (CSS) is a well-developed CO₂ elimination technology affixed to CO₂ emission sources. It comprises three stages: CO₂ is captured from flue gas, then shipped and stored underground [6]. Amine scrubbing is one of the most common CCS technologies commercialized and applied industrially. However, it suffers from several limitations, including amine chemical degradation, equipment corrosion, and high energy requirement for amine regeneration [3]. In this regard, physisorption-based CO₂ capture provides a potential replacement based on its simplicity, economic scale, and low energy requirement. Varieties of physical adsorbents, including zeolites and activated carbon, have been evaluated for CO₂ gas capture.

Compared to these traditional adsorbent materials, metal–organic frameworks (MOF) are distinguished by their extraordinarily high surface area and porosity, together with their flexibility in framework formation. They are an organic–inorganic hybrid formed from a metal precursor and an organic ligand [7]. In contrast to rigid zeolite and activated carbon materials, their adjustability and flexibility in pore structure and framework building have enabled them to replace traditional adsorbents. Moreover, their superior adsorption characteristic, rapid adsorption kinetics, and reversibility suggest they are a promising adsorbent material [8].

MIL-101(Cr) is an attractive type of MOF for serving as a CO₂ adsorbent due to its many outstanding features for adsorption, including high surface area, large pore volume, and excellent chemical and thermal strength [9,10]. There is an abundance of published studies relevant to the use of MIL-101(Cr) in CO₂ adsorption. Hong et al. [11] carried out a comparative study to determine the adsorptive properties of 13X zeolite monoliths and MIL-101(Cr) monoliths for CO₂ adsorption. The MIL-101(Cr) was fabricated using a hydrothermal reaction in this work, and the results showed that the CO₂ capture performance of MIL-101(Cr) monoliths was better than that of zeolite monoliths. Zhang et al. [12] successfully synthesized MIL-101(Cr) composites with a solvent-based hydrothermal method for CO₂ adsorption in 2019. In the same year, Yulia et al. [13] reported the fabrication of MIL-101(Cr) using a fluorine-free hydrothermal method, and achieved a CO₂ adsorption capacity of 2.28 mmol/g at a temperature of 298 K and pressure of 600 KPa.

Most of these studies adopted the hydrothermal method to synthesize the MIL-101(Cr) for CO₂ adsorption. To the best of our knowledge, none of the studies to date studying the CO₂ adsorption ability of MIL-101(Cr) used a solvent-free fabrication method. In addition, relevant scientific studies using solvent-free methods to synthesize MIL-101(Cr) are still lacking.

The most common MOF synthesis method applied in the laboratory is hydrothermal (solvothermal), but this method requires a massive amount of solvent, which is most probably toxic, during the organic linkage reaction. Furthermore, it can cause environmental issues and make the upscaling process challenging and expensive [14]. Therefore, in this study, we employed a solvent-free method for synthesizing MIL-101(Cr) to investigate its potential in CO₂ adsorption. Mechanochemical fabrication is a solvent-free MOF fabrication method that uses force to grind the mixture of starting materials in order to initiate the reaction [15]. It is the most simple, economical, and green technique for synthesizing MOF compared to the methods involving organic solvents.

In the present study, MIL-101(Cr) was fabricated using a solvent-free method in order to develop a clean and efficient way of synthesizing MOF. A total of seven MIL-101(Cr) samples with different Cr to organic linker molar ratios were prepared in order to investigate the influence of the molar ratio of starting materials on the MIL-101(Cr) MOF's CO₂ adsorption capacities.

2. Materials and Methods

2.1. Solvent-Free Preparation of MIL-101(Cr)

We purchased 99% pure chromium trinitrate nonahydrate (Cr(NO₃)₃·9H₂O) and 98% pure 1,4-benzene dicarboxylate (BDC) from Sigma-Aldrich, St. Louis, MO, USA. VWR International supplied ethanol (EtOH, 99%). Cr(NO₃)₃·9H₂O and BDC were used as the metal precursor and organic linker, respectively, for the synthesis of MIL-101(Cr). The method we used solvent-free synthesis of chromium-based MIL-101 MOF is similar to the procedures reported by [16], with minor modifications. First, the weighed amounts of starting materials, Cr(NO₃)₃·9H₂O and BDC, were mixed and ground for around 30 min at room temperature. The resulting mixture was then transferred into a stainless-steel, Teflon-lined autoclave and heated at 220 °C for 4 h. After, it was washed with hot ethanol at 60 °C to eliminate any unreacted reactants. Then, the MIL-101(Cr) solid was recovered by 15 min centrifugation at 5500 rpm. Lastly, the obtained green MIL-101(Cr) powder was dried in an oven at 120 °C overnight. The color changes of MIL-101(Cr) that occurred along the solvent-free synthesis process are demonstrated in Figure S1.

2.2. Characterization Techniques

All the samples were scanned with a Shimadzu Model 6000 diffractometer (Shimadzu, Kyoto, Japan) over the 2θ angle ranging from 5° to 30° at a scan rate of 2°/min with Cu-Kα radiation to obtain their XRD patterns. The morphology and the elemental composition of the samples were obtained with Hitachi S-3400N scanning electron microscopy (SEM), coupled with energy-dispersive X-ray spectroscopy (EDX). The samples' Fourier transform infrared (FTIR) spectra were obtained using a Nicolet iS10 instrument. Each sample was scanned from wavenumbers in the region of 400–4000 cm⁻¹, with a 1 cm⁻¹ interval. Thermal stability analysis of the samples was performed using a PerkinElmer STA 8000 simultaneous thermal analyzer. The samples were exposed to an increasing temperature condition from 50 to 800 °C at a heating rate of 10 °C/min, with the N₂ flow rate kept constant at 20 mL/min during the thermogravimetric analysis. The samples' surface textural properties, including the BET surface area, average pore size, and total pore volume, were obtained from N₂ adsorption isotherms at 350 °C on a Micromeritics 3Flex surface characterization analyzer. All the samples were degassed at 150 °C with N₂ gas before the analysis.

2.3. CO₂ Adsorption Test Setup

Figure 1 illustrates the setup for determining the CO₂ gas adsorption capacity of the MIL-101(Cr) synthesized at room temperature using this procedure. Before each experiment, the sample was degassed at 120 °C overnight. After the degasification, a weighed sample was inserted into a porous bag and placed in a stainless-steel vessel. Subsequently, the gas valve was turned on to allow pure CO₂ to flow into the adsorption vessel and fill it up. The concentration of the purging CO₂ gas was measured by a CO₂ meter (AZ-001). After each experiment run (30 min), the sample was weighed to obtain its final weight after the adsorption. The CO₂ adsorption capacity for each sample was calculated by:

$$n_{ads} = \left(\frac{W_f - W_i}{W_i} \right) \div M_{CO_2} \quad (1)$$

$$Q_{ads} = \frac{n_{ads}}{(W_i \div 1000)} \quad (2)$$

where n_{ads} is millimoles of adsorbed CO_2 (mmol); W_i is the weight of sample before the adsorption test (mg); W_f is the weight of sample after the adsorption test (mg); M_{CO_2} is the molar mass of CO_2 (44.009 mg/mmol); Q_{ads} is the adsorption capacity (mmol/g).

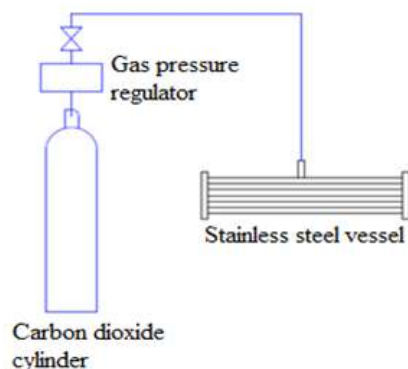


Figure 1. Setup for measuring CO_2 adsorption capacity.

3. Results and Discussion

3.1. Characterization of MIL-101(Cr)

The XRD patterns of the MIL-101(Cr) synthesized using the solvent-free method in Figure 2 are in agreement with those reported in the literature [16,17], confirming the successful formation of pure MIL-101(Cr). The diffraction peak became stronger as the Cr to BDC molar ratio increased. The breadth of the diffraction peak is related to the particle size, where a broader peak indicates a smaller particle [18]. Hence, the XRD patterns indicated that the size of MIL-101(Cr) solids decreased as the molar ratio between Cr and BDC linker increased. Therefore, the sample with a molar ratio of 2.5:1 exhibited the smallest particle size as it had a broader diffraction peak.

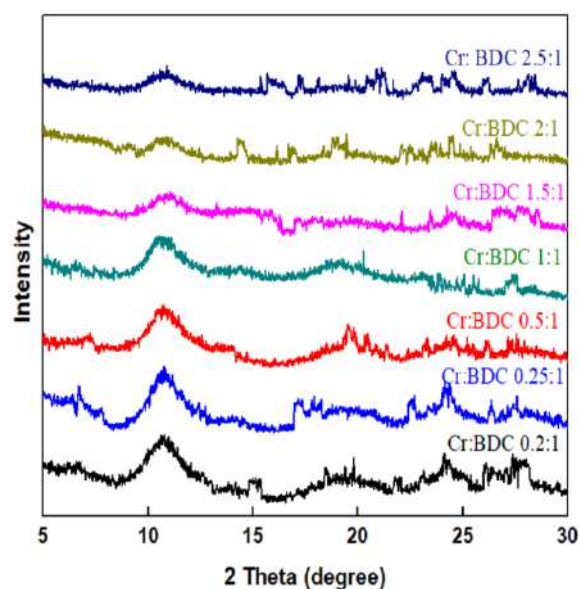


Figure 2. XRD patterns of the Cr-based MIL-101 MOF synthesized in this work.

The surface morphology of the synthesized MIL-101(Cr) is shown in Figure 3. As the molar ratio of Cr to BDC organic linker increased, one can notice the increase in the surface roughness of the MIL-101(Cr). The increased surface roughness is associated with reduced particle size. Based on the SEM images in Figure 3a–c, we observed that the particle size of MIL-101(Cr) decreased as a higher Cr to BDC molar ratio was employed. The SEM image of the sample with a Cr:BDC molar ratio of 1.5:1 (Figure 3e) shows that

it consisted of small, irregularly shaped particles. When the molar ratio was decreased from 1.5:1 to 1:1, we observed fine growth of small, irregular, granular-shaped particles in an aggregation state (Figure 3d). The findings are similar to the MIL-101(Cr) morphology reported elsewhere [16,17], indicating that MIL-101(Cr) can grow well using the solvent-free method with an equal molar ratio of Cr to BDC organic linker. The surface of MIL-101(Cr) with 2:1 and 2.5:1 Cr to BDC molar ratio was found to have many regular round-shaped particles, as shown in Figure 3f,g, respectively. These round-shaped particles are thought to be the unreacted chromium particles [19] due to an excess in chromium metal reactant when a high ratio of Cr over BDC linker is utilized during the crystallization reaction. Proper manipulation of the amount of Cr and BDC organic linker used during the solvent-free reaction is vital for the growth of the desired morphology of Cr-based MIL-101 MOF.

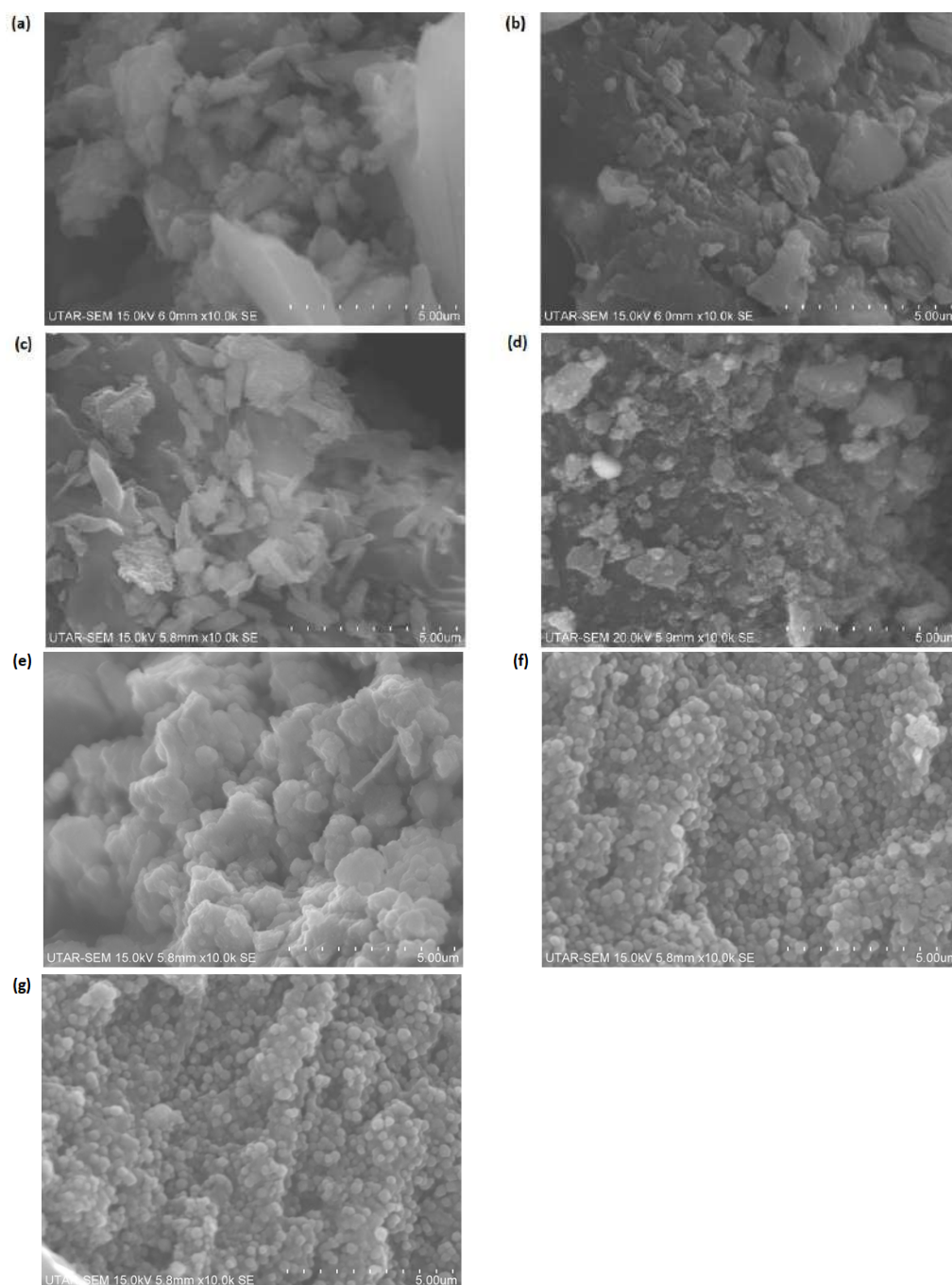


Figure 3. SEM images of MIL-101(Cr) with different Cr: BDC molar ratios: (a) 0.2:1, (b) 0.25:1, (c) 0.5:1, (d) 1:1, (e) 1.5:1, (f) 2:1, and (g) 2.5:1.

The elemental composition of each variant of MIL-101(Cr) synthesized in this work was determined using EDX analysis and is presented in Table 1. Cr was successfully incorporated into all samples regardless of the Cr-to-BDC molar ratio. The carbon and oxygen elements within the samples were sourced from BDC organic linkers that participated in the formation of MIL-101(Cr) [16]. A higher Cr-to-BDC molar ratio used during the organic linkage reaction is supposed to have a higher weight percentage of Cr element in the sample, but the EDX analysis showed that the sample with a Cr-to-BDC molar ratio of 0.5:1 had a lower Cr content than the sample with a Cr-to-BDC molar ratio of 0.25 to 1. This could be due to the improper substitution of Cr within the 0.5:1 molar ratio MIL-101(Cr). However, the overall EDX analysis result for the MIL-101(Cr) synthesized in this work is in line with the changes in the Cr to BDC molar ratio used.

Table 1. The weight percentage of chromium, carbon, and oxygen elements of MIL-101(Cr) synthesized in this work.

Cr to BDC Molar Ratio	Cr (wt %)	C (wt %)	O (wt %)
0.2:1	24.22	42.74	33.05
0.25:1	26.28	40.73	32.99
0.5:1	22.01	45.79	32.21
1:1	27.52	41.45	31.02
1.5:1	29.10	37.83	33.07
2:1	33.07	29.52	37.41
2.5:1	35.27	30.05	34.69

The results of the FTIR analysis conducted on the MIL-101(Cr) in Figure 4 are in accordance with the literature data [16–18], particularly in the fingerprint region between 400 and 1500 cm^{-1} . An intense absorption band around 520 cm^{-1} occurred due to the chromium-to-oxygen stretching vibration [18]. Most of the absorption bands at the region between 600 and 1600 cm^{-1} belonged to the functional groups and the benzene ring within the BDC organic linker that participated in the formation of MIL-101(Cr) [18]. The strong peak at 720 cm^{-1} was attributed to the mono-substituted benzene ring [17], while the peak at 750 cm^{-1} was the vibration of the C–H group [18]. In addition, the peaks around 1390 and 1450 cm^{-1} were due to the symmetrical vibration of the O–C–O of the benzene ring and the dicarboxylate functional group, respectively, within the BDC [20]. A peak at 1640 cm^{-1} was due to the presence of adsorbed water within the pores of the synthesized MIL-101(Cr) after exposure to air. Since the absorption band observed at 1715 cm^{-1} is due to the unreacted BDC [18], this peak was stronger in the samples that used a higher BDC content relative to the Cr.

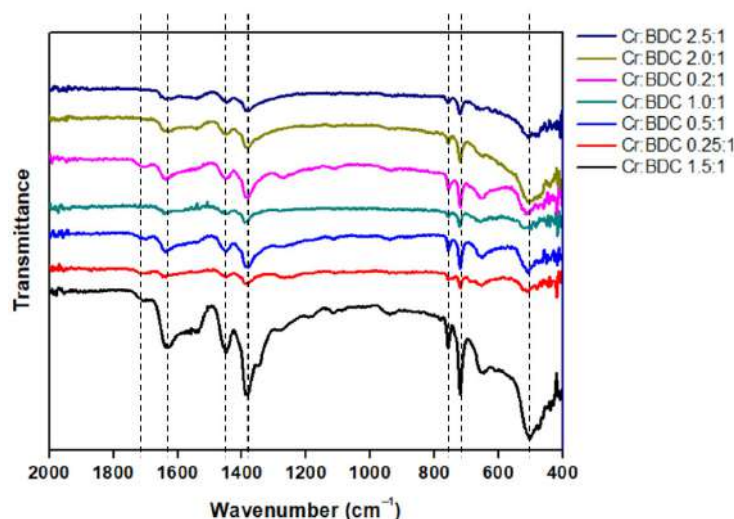


Figure 4. FTIR spectra of different MIL-101(Cr) variants synthesized in this work.

3.2. Textural Properties of MIL-101(Cr)

The N₂ adsorption and desorption isotherms at 350 °C for the Cr-based MIL-101 MOF synthesized in this work are displayed in Figure 5. It shows a Type I(b) isotherm according to IUPAC categorization [21]. The N₂ adsorption and desorption branches coincide well; no obvious hysteresis loop was observed, indicating there was no large pore structure within the sample. We observed that secondary uptake happened at a relative pressure (P/P₀) of around 0.1 to 0.2 [22,23], as shown in Figure 6. This occurrence was mainly due to the existence of two kinds of mesoporous windows within the MIL-101(Cr). The two mesoporous structures were the pentagonal windows with a diameter of 2.9 nm, and the hexagonal windows with a diameter of 3.4 nm [24,25].

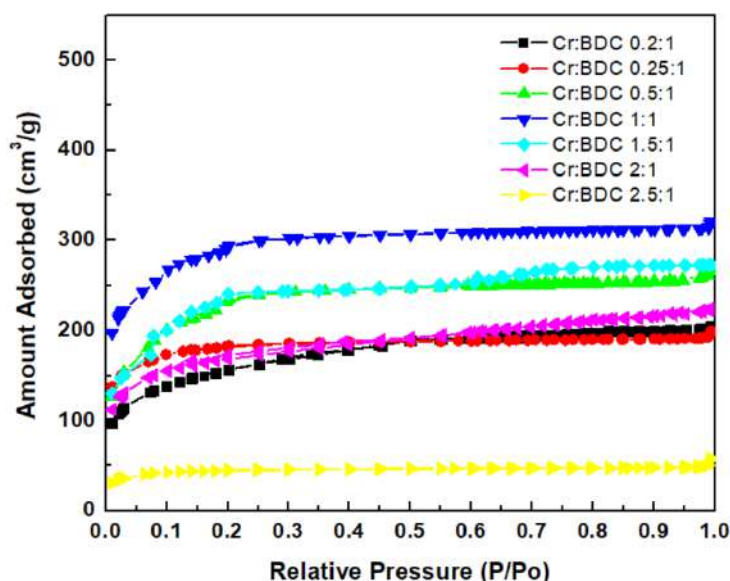


Figure 5. N₂ adsorption and desorption isotherms of chromium-based MIL-101 MOF synthesized in this work.

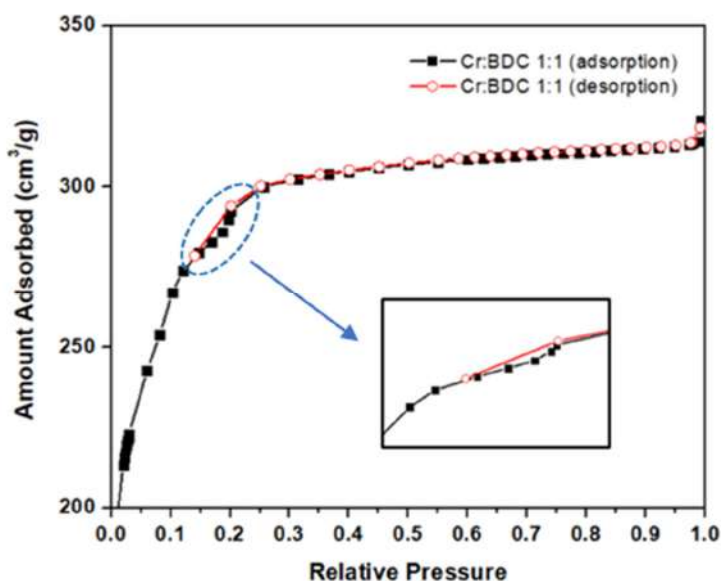


Figure 6. Nitrogen adsorption/desorption isotherm for the MIL-101(Cr) with a Cr:BDC molar ratio of 1:1 synthesized in this work. Inset: The secondary uptake portion is enlarged in the inset.

The detailed textural properties of the MIL-101(Cr) synthesized in this work are summarized in Table 2. The sample with a Cr to BDC molar ratio of 1:1 achieved the

highest BET surface area of 1110.1 m²/g. Although its average pore diameter (1.8 nm) was the smallest among the samples synthesized, its pore volume was the highest, attaining a 0.5 cm³/g total pore volume. Its CO₂ adsorption capacity was the best compared to the other Cr o-BDC molar ratios. The lowest BET surface area and total pore volume were found in the MIL-101(Cr) with a Cr-to-BDC molar ratio of 2.5:1: only 178.6 m²/g and 0.1 cm³/g, respectively. Correspondingly, its adsorption capacity was the lowest compared to the other samples. High surface area and pore volume coupled with smaller pore diameter are favorable for the adsorption mechanism. Hence, the textural properties of the MIL-101(Cr) MOF synthesized in this work align with the CO₂ adsorption capacity result. The average pore diameter of MIL-101(Cr) ranged from 1.8 to 2.5 nm.

Table 2. Textural properties and CO₂ adsorption capacity of MIL-101(Cr) synthesized in this work.

Cr:BDC Molar Ratio	S_{BET} ¹ (m ² /g)	Average Pore Diameter ² (nm)	Pore Volume ³ (cm ³ /g)	Q_{ads} ⁴ (mmol/g)
0.2:1	565.6	2.5	0.3	8.1
0.25:1	705.2	1.8	0.3	10.5
0.5:1	856.1	1.8	0.4	18
1:1	1110.1	1.8	0.5	18.8
1.5:1	728.2	2.3	0.4	18
2:1	636.8	2.2	0.3	9.4
2.5:1	178.6	2.0	0.1	1.2

¹ BET surface area obtained in a P/P₀ range of 0.05 to 0.15. ² Average pore diameter calculated by the BET method. ³ Total pore volume at a P/P₀ of ~0.9. ⁴ Adsorption capacity of CO₂.

3.3. Thermogravimetric Analysis (TGA) of MIL-101(Cr)

The thermal stability test results of the synthesized MIL-101(Cr) are presented in Figure 7. As shown, all chromium-based MIL-101 MOFs experienced two weight losses during the thermal decomposition process, consistent with the reference works [7,16,26,27]. The first weight loss happened from room temperature to 200 °C, which could be ascribed to the loss of adsorbed water molecules, unreacted organic matter, and residual washing solvent [16,26,27]. Since all the samples were dried at 80 °C overnight before undergoing the TGA analysis, a small degree of weight loss occurred at the first stage. The second phase of weight loss occurred between 200 and 500 °C. At this stage, significant weight loss was observed due to the breakdown of the MIL-101(Cr) framework structure [16,26,27]. In short, the MIL-101(Cr) synthesized in this work generally exhibited high thermal stability for temperatures up to 350 °C.

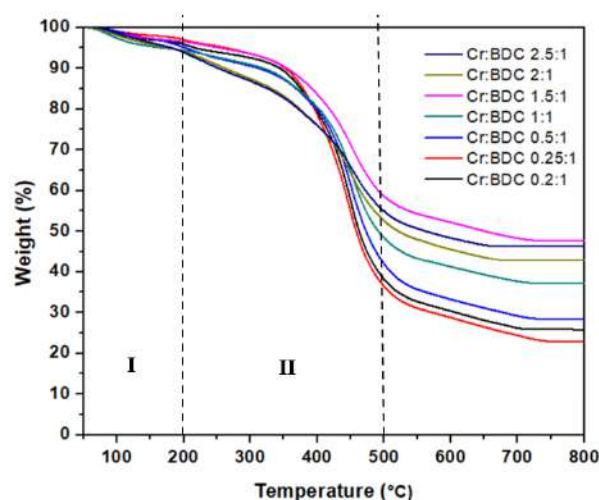


Figure 7. TGA curves of the MIL-101(Cr) synthesized in this work.

The total weight loss for the second phase of decomposition is presented in Table 3. As shown, the MIL-101(Cr) with a Cr-to-BDC molar ratio of 0.25 to 1 experienced the most severe weight loss during the second stage decomposition, up to 62.23%. In contrast, the weight loss percentage for MIL-101(Cr) with a Cr-to-BDC molar ratio of 1.5:1 was the lowest, indicating that it had the most robust structure of the samples considered.

Table 3. Total weight loss of MIL-101(Cr) during the second stage of decomposition.

Cr-to-BDC Molar Ratio	Initial Weight ¹ (mg)	Final Weight ² (mg)	Total Weight Loss (%)
0.2:1	14.88	5.92	60.22
0.25:1	14.51	5.48	62.23
0.5:1	19.79	8.75	55.79
1:1	17.96	9.20	48.78
1.5:1	23.58	14.34	39.19
2:1	17.81	9.98	43.96
2.5:1	15.92	9.34	41.33

¹ Initial weight during 2nd stage of weight loss at 200 °C. ² Final weight during 2nd stage of weight loss at 500 °C.

3.4. CO₂ Adsorption Capacity

Table 4 shows the CO₂ gas adsorption test conducted at room temperature for the MIL-101(Cr) synthesized in this work. The CO₂ adsorption for the samples with the lowest Cr-to-BDC molar ratio (0.2:1) was found to be 8.1 mmol/g. The CO₂ adsorption capacity, however, improved as the molar ratio of metal precursor and organic ligand increased from 0.2:1 to 1:1. The MIL-101(Cr) with an equal Cr-to-BDC molar ratio was the best-performing sample, attaining 18.8 mmol/g, whereas the MIL-101(Cr) with 2.5:1 exhibited the lowest adsorption capacity of only 1.2 mmol/g.

Table 4. CO₂ gas adsorption result of the MIL-101(Cr) synthesized in this work.

Cr-to-BDC Molar Ratio	W _i ¹ (mg)	W _f ² (mg)	n _{ads} ³ (mmol)	Q _{ads} ⁴ (mmol/g)
0.2:1	1091.0 ± 57.8	1479.1 ± 81.4	8.8 ± 0.4	8.1 ± 0.5
0.25:1	907.5 ± 44.5	1325.2 ± 70.2	9.5 ± 0.5	10.5 ± 0.6
0.5:1	918.5 ± 52.4	1646.1 ± 79.0	16.5 ± 1.0	18.0 ± 0.9
1:1	903.9 ± 47.0	1650.7 ± 94.1	17.0 ± 1.0	18.8 ± 1.1
1.5:1	922.3 ± 52.6	1654.3 ± 97.6	16.6 ± 0.8	18.0 ± 1.0
2:1	1429.5 ± 77.2	2021.0 ± 97.0	13.4 ± 0.7	9.4 ± 0.6
2.5:1	1317.0 ± 63.2	1388.4 ± 75.0	1.6 ± 0.1	1.2 ± 0.1

¹ Initial weight before adsorption test. ² Final weight after adsorption test. ³ Millimoles of adsorbed CO₂. ⁴ Adsorption capacity of CO₂.

It is well-known that the high surface area of MOFs leads to a high CO₂ adsorption capacity. Figure 8 illustrates the relationship between the textural properties of MIL-101(Cr) variants and their CO₂ adsorption capacity. It is clear that the CO₂ adsorption capacity was significantly affected by the textural properties of MIL-101(Cr). Owing to its highest surface area and pore volume, the MIL-101(Cr) with an equal Cr to BDC molar ratio demonstrated the highest CO₂ adsorption capacity amongst all the samples.

Table 5 compares the CO₂ adsorption capacity of MIL-101(Cr) synthesized in this work with the other data obtained from the literatures [1,10,22,23,28]. The CO₂ adsorption capacity of our MIL-101(Cr) is relatively higher than that reported in many studies. Although our CO₂ adsorption capacity is lower than that reported by Zhou et al. [28], our testing conditions are more economical as tests are performed at only 1 bar.

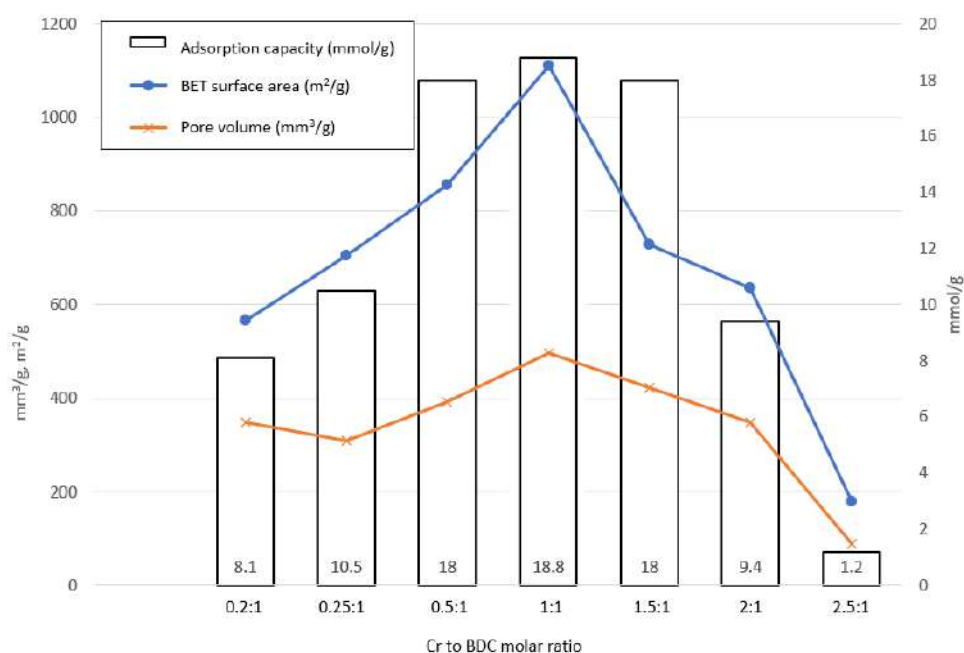


Figure 8. Relationship between CO₂ adsorption capacity, total pore volume, and BET specific surface area of the MIL-101(Cr) synthesized in this work.

Table 5. CO₂ gas adsorption capacities of MIL-101(Cr) reported in various works.

MOF Name	Temperature (K)	Pressure (bar)	Adsorption Capacity (mmol/g)	Reference
MIL-101(Cr)	298	6	2.28	[1]
MIL-101(Cr)	298	7	9.72	[10]
MIL-101(Cr)	273	1	5.77	[22]
MIL-101(Cr)	298	1	7.7	[23]
MIL-101(Cr)	298	25	22.4	[28]
MIL-101(Cr) (1:1)	298	1	18.8	This work

The reversibility of MIL-101(Cr) adsorption and its regeneration ability are key factors for evaluating it as an efficient CO₂ adsorbent. The regeneration of an adsorbent can be achieved by several methods, including temperature swing adsorption (TSA), pressure swing adsorption (PSA), vacuum swing adsorption (VSA), vacuum temperature swing adsorption (VTSA), and steam stripping [29].

The regenerative ability of MIL-101(Cr) has been previously investigated and optimized by other researchers. Five consecutive cycles of TSA adsorption–desorption were performed with MIL-101(Cr) by Ye et al. [30]. In this adsorption–desorption test, regeneration was carried out by increasing the temperature to 100 °C, with N₂ purging after the complete adsorption test. It was found that the adsorption capacity for each test cycle remained almost unchanged, indicating its adsorption was reversible, and MIL-101(Cr) could be easily regenerated. Soltanolkotabi et al. [23] also reported that MIL-101(Cr) could retain its CO₂ adsorption capacity even after more than 100 cycles of adsorption–desorption testing.

4. Conclusions

In this study, a green and solvent-free method was employed to synthesize chromium-based MIL-101 MOF for CO₂ adsorption. The molar ratio of the starting materials (Cr and BDC) and textural properties were found to play an essential role in determining the CO₂ adsorption capacity of MIL-101(Cr) at room temperature. Our results indicated that the MIL-101(Cr) made of an equal Cr-to-BDC molar ratio was the best sample and achieved an

excellent CO₂ adsorption capacity of 18.8 mmol/g. The adsorption capacity is also higher compared to the values reported in the literature, indicating it is a superior adsorbent for CO₂ removal.

Supplementary Materials: The following are available online at <https://www.mdpi.com/article/10.3390/su14031152/s1>, Figure S1: Color changes along the synthesis of MIL-101(Cr).

Author Contributions: Conceptualization, K.C.C. and S.O.L.; methodology, S.-Y.L. and P.S.H.; validation, S.S.L., W.J.L. and B.S.O.; formal analysis, P.S.H.; investigation, P.S.H.; resources, K.C.C.; data curation, P.S.H.; writing—original draft preparation, P.S.H.; writing—review and editing, K.C.C., W.J.L. and S.O.L.; visualization, S.S.L.; supervision, K.C.C. and S.O.L.; project administration, K.C.C. and S.S.L.; funding acquisition, K.C.C. All authors have read and agreed to the published version of the manuscript.

Funding: This research was funded by Universiti Tunku Abdul Rahman under UTAR Research Fund (UTARRF), grant number IPSR/RMC/UTARRF/2020-C2/C05.

Institutional Review Board Statement: Not applicable.

Informed Consent Statement: Not applicable.

Data Availability Statement: All the data are available inside this paper and in the Supplementary Materials.

Conflicts of Interest: The authors declare no conflict of interest. The funders had no role in the design of the study; in the collection, analyses, or interpretation of data; in the writing of the manuscript; or in the decision to publish the results.

References

1. Yulia, F.; Nasruddin; Zulys, A.; Ruliandini, R. Metal-organic framework based chromium terephthalate (MIL-101 Cr) growth for carbon dioxide capture: A review. *J. Adv. Res. Fluid Mech. Therm. Sci.* **2019**, *57*, 158–174.
2. Yoro, K.O.; Daramola, M.O. CO₂ emission sources, greenhouse gases, and the global warming effect. In *Advances in Carbon Capture*; Woodhead Publishing: Pretoria, South Africa, 2020; pp. 3–28.
3. Hu, Z.; Wang, Y.; Shah, B.B.; Zhao, D. CO₂ capture in metal-organic framework adsorbents: An engineering perspective. *Adv. Sustain. Syst.* **2019**, *3*, 1800080. [[CrossRef](#)]
4. Gregory, J.M.; White, N.J.; Church, J.A.; Bierkens, M.F.P.; Box, J.E.; van den Broeke, M.R.; Cogley, J.G.; Fettweis, X.; Hanna, E.; Huybrechts, P.; et al. Twentieth-century global-mean sea level rise: Is the whole greater than the sum of the parts? *J. Clim.* **2013**, *26*, 4476–4499. [[CrossRef](#)]
5. Peterman, K.E. Climate change literacy and education: History and project overview. *ACS Symp. Series* **2017**, *1247*, 1–14.
6. Yu, J.; Xie, L.H.; Li, J.R.; Ma, Y.; Seminario, J.M.; Balbuena, P.B. CO₂ capture and separations using MOFs: Computational and experimental studies. *Chem. Rev.* **2017**, *117*, 9674–9754. [[CrossRef](#)]
7. Kooti, M.; Pourreza, A.; Rashidi, A. Preparation of MIL-101 nanoporous carbon as a new type of nanoadsorbent for HS removal from gas stream. *J. Nat. Gas Sci. Eng.* **2018**, *57*, 331–338. [[CrossRef](#)]
8. Bahri, M.; Haghighat, F.; Kazemian, H.; Rohani, S. A comparative study on metal organic frameworks for indoor environment application: Adsorption evaluation. *Chem. Eng. J.* **2017**, *313*, 711–723. [[CrossRef](#)]
9. Bhattacharjee, S.; Chen, C.; Ahn, W.S. Chromium terephthalate metal-organic framework MIL-101: Synthesis, functionalization, and applications for adsorption and catalysis. *RSC Adv.* **2014**, *4*, 52500–52525. [[CrossRef](#)]
10. Montazerolghaem, M.; Aghamiri, S.F.; Talaie, M.R.; Tangestaninejad, S. A comparative investigation of CO₂ adsorption on powder and pellet forms of MIL-101. *J. Taiwan Inst. Chem. Eng.* **2017**, *72*, 45–52. [[CrossRef](#)]
11. Hong, W.Y.; Perera, S.P.; Burrows, A.D. Comparison of MIL-101(Cr) metal-organic framework and 13X zeolite monoliths for CO₂ capture. *Micropor. Mesopor. Mat.* **2020**, *308*, 110525. [[CrossRef](#)]
12. Zhang, X.T.; Li, F.Q.; Ren, J.X.; Guan, Z.Z.; Zhang, L.J.; Feng, H.J.; Hou, X.; Ma, C. Preparation and CO₂ breakthrough adsorption of MIL-101(Cr)-D composites. *J. Nanopart. Res.* **2019**, *21*, 105. [[CrossRef](#)]
13. Yulia, F.; Utami, V.J.; Nasruddin; Zulys, A. Synthesis, characterizations, and adsorption isotherms of CO₂ on chromium terephthalate (MIL-101) metal-organic frameworks (MOF). *Int. J. Technol.* **2019**, *10*, 1427–1436. [[CrossRef](#)]
14. Bo, Q.B.; Pang, J.J.; Wang, H.Y.; Fan, C.H.; Zhang, Z.W. Hydrothermal synthesis, characterization and photoluminescent properties of the microporous metal organic frameworks with 1,3-propanediaminetetraacetate ligand and its auxiliary ligand. *Inorg. Chim. Acta* **2015**, *428*, 170–175. [[CrossRef](#)]
15. Pilloni, M.; Padella, F.; Ennas, G.; Lai, S.; Bellusci, M.; Rombi, E.; Sini, F.; Pentimalli, M.; Delitala, C.; Scano, A.; et al. Liquid-assisted mechanochemical synthesis of an iron carboxylate metal organic framework and its evaluation in diesel fuel desulfurization. *Micropor. Mesopor. Mat.* **2015**, *213*, 14–21. [[CrossRef](#)]

16. Leng, K.; Sun, Y.; Li, X.; Sun, S.; Xu, W. Rapid synthesis of metal-organic frameworks MIL-101(Cr) without the addition of solvent and hydrofluoric acid. *Cryst. Growth Des.* **2016**, *16*, 1168–1171. [[CrossRef](#)]
17. Utami, V.J.; Yulia, F.; Nasruddin; Budiyanto, M.A.; Zulys, A. CO₂/N₂ adsorption selectivity using metal-organic framework MIL-101(Cr) for marine engine exhaust model. *AIP Conf. Proc.* **2020**, *2255*, 060035.
18. Shafiei, M.; Alivand, M.S.; Rashidi, A.; Samimi, A.; Mohebbi-Kalhari, D. Synthesis and adsorption performance of a modified micro-mesoporous MIL-101(Cr) for VOCs removal at ambient conditions. *Chem. Eng. J.* **2018**, *341*, 164–174. [[CrossRef](#)]
19. Satgurunathan, T.; Bhavan, P.S.; Joy, R.D.S. Green synthesis of chromium nanoparticles and their effects on the growth of the prawn macrobrachium rosenbergii post-larvae. *Biol. Trace Elem. Res.* **2019**, *187*, 543–552. [[CrossRef](#)]
20. Huang, X.L.; Hu, Q.; Gao, L.; Hao, Q.R.; Wang, P.; Qin, D.L. Adsorption characteristics of metal-organic framework MIL-101(Cr) towards sulfamethoxazole and its persulfate oxidation regeneration. *RSC Adv.* **2018**, *8*, 27623–27630. [[CrossRef](#)]
21. Thommes, M.; Kaneko, K.; Neimark, A.V.; Olivier, J.P.; Rodriguez-Reinoso, F.; Rouquerol, J.; Sing, K.S.W. Physisorption of gases, with special reference to the evaluation of surface area and pore size distribution (IUPAC technical report). *Pure Appl. Chem.* **2015**, *87*, 1051–1069. [[CrossRef](#)]
22. Zhao, T.; Li, S.H.; Shen, L.; Wang, Y.; Yang, X.Y. The sized controlled synthesis of MIL-101(Cr) with enhanced CO₂ adsorption property. *Inorg. Chem. Commun.* **2018**, *96*, 47–51. [[CrossRef](#)]
23. Soltanolkotabi, F.; Talaie, M.R.; Aghamiri, S.; Tangestaninejad, S. Introducing a dual-step procedure comprising microwave and electrical heating stages for the morphology-controlled synthesis of chromium-benzene dicarboxylate, MIL-101(Cr), applicable for CO₂ adsorption. *J. Environ. Manag.* **2019**, *250*, 109416. [[CrossRef](#)] [[PubMed](#)]
24. Zhou, Z.; Mei, L.; Ma, C.; Xu, F.; Xiao, J.; Xia, Q.; Li, Z. A novel bimetallic MIL-101(Cr, Mg) with high CO₂ adsorption capacity and CO₂/N₂ selectivity. *Chem. Eng. Sci.* **2016**, *147*, 109–117. [[CrossRef](#)]
25. Ferey, G.; Mellot-Draznieks, C.; Serre, C.; Millange, F.; Dutour, J.; Surble, S.; Margiolaki, I. A chromium terephthalate-based solid with unusually large pore volumes and surface area. *Science* **2005**, *309*, 2040–2042. [[CrossRef](#)] [[PubMed](#)]
26. Zhao, H.; Li, Q.; Wang, Z.; Wu, T.; Zhang, M. Synthesis of MIL-101(Cr) and its water adsorption performance. *Micropor. Mesopor. Mat.* **2020**, *297*, 110044. [[CrossRef](#)]
27. Rallapalli, P.B.S.; Raj, M.C.; Senthikumar, S.; Somani, R.S.; Bajaj, H.C. HF-free synthesis of MIL-101(Cr) and its hydrogen adsorption studies. *Environ. Prog. Sustain. Energy* **2016**, *35*, 461–468. [[CrossRef](#)]
28. Zhou, X.; Huang, W.; Miao, J.; Xia, Q.; Zhang, Z.; Wang, H.; Li, Z. Enhanced separation performance of a novel composite material GrO@MIL-101 for CO₂/CH₄ binary mixture. *Chem. Eng. J.* **2014**, *266*, 339–344. [[CrossRef](#)]
29. Liu, Q.; Ning, L.; Zheng, S.; Tao, M.; Shi, Y.; He, Y. Adsorption of carbon dioxide by MIL-101(Cr): Regeneration conditions and influence of flue gas contaminants. *Sci. Rep.* **2013**, *3*, 2916. [[CrossRef](#)] [[PubMed](#)]
30. Ye, S.; Jiang, X.; Ruan, L.W.; Liu, B.; Wang, Y.M.; Zhu, J.F.; Qiu, L.G. Post-combustion CO₂ capture with the HKUST-1 and MIL-101(Cr) metal-organic frameworks: Adsorption, separation and regeneration investigations. *Micropor. Mesopor. Mat.* **2013**, *179*, 191–197. [[CrossRef](#)]